A vestige low metallicity gas shell surrounding the radio galaxy 0943–242 at $z = 2.92$

L. Binette[1]**, J.D. Kurk**[2]**, M. Villar-Martín**[3]**, and H.J.A. Röttgering**[2]

[1] Instituto de Astronomía, UNAM, Ap. 70-264, 04510 México, DF, México (binette@astroscu.unam.mx)
[2] Leiden Observatory, P.O. Box 9513, 2300 RA, Leiden, The Netherlands
[3] Department of Physical Sicences, University of Hertfordshire, College Lane, Hatfield Herts, AL10 9AB, UK

Abstract. Observations are presented showing the doublet C IV $\lambda\lambda$1548, 1551 absorption lines superimposed on the C IV emission in the radio galaxy 0943–242. Within the errors, the redshift of the absorption system that has a column density of $N_{CIV} = 10^{14.5\pm0.1}$ cm^{-2} coincides with that of the deep Lyα absorption trough observed by Röttgering et al. (1995). The gas seen in absorption has a resolved spatial extent of at least 13 kpc (the size of the extended emission line region). We first model the absorption and emission gas as co-spatial components with the same metallicity and degree of excitation. Using the information provided by the emission and absorption line ratios of C IV and Lyα, we find that the observed quantities are incompatible with photoionization or collisional ionization of cloudlets with uniform properties. We therefore reject the possibility that the absorption and emission phases are co-spatial and favour the explanation that the absorption gas has low metallicity and is located further away from the host galaxy (than the emission line gas). The larger size considered for the outer halo makes plausible the proposed metallicity drop relative to the inner emission gas. In absence of confining pressure comparable to that of the emission gas, the outer halo of 0943–242 is considered to have a very low density allowing the metagalactic ionizing radiation to keep it higly ionized. In other radio galaxies where the jet has pressurized the outer halo, the same gas would be seen in emission (since the emissivity scales as n_H^2) and not in absorption as a result of the lower filling factor of the denser condensations. This would explain the anticorrelation found by van Ojik et al. (1997) between Lyα emission sizes (or radio jet sizes) and the observation (or not) of H I in absorption. The estimated low metallicity for the absorption gas in 0943–242 ($Z \sim 0.01Z_\odot$) and its proposed location –outer halo outside the radio cocoon– suggest that its existence preceeds the observed AGN phase and is a vestige of the initial starburst at the onset of formation of the parent galaxy.

Key words: galaxies: individual: 0943–242 – cosmology: early Universe – galaxies: active – galaxies: formation – galaxies: ISM

1. Introduction

Very high redshift ($z > 2$) radio galaxies (hereafter HZRG) show emission lines of varying degree of excitation. In virtually all objects, the Lyα line is the strongest and is usually accompanied by high excitation lines of C IV $\lambda\lambda$1549, C III]λ1909, He II λ1640 and, at times, N Vλ1240 (Röttgering et al. 1997 and references therein). An important characteristic of the emission gas is its spatial scale. The sizes of the Lyα emission region range from 15 to 120 kpc (van Ojik et al. 1997).

Most ground work on HZRG is performed at rather low resolution ($\sim$ 20Å) to maximize the probability of line detection and the S/N. However a very potent discovery was made by van Ojik et al. (1997, hereafter vO97) at much higher resolution, that of extended H I *absorption* gas. In effect, out of 18 HZRG spectra taken at the unusually high resolution of $\simeq$ 1.5–3Å, vO97 found –in 60% of the objects– deep absorption troughs superimposed on the Lyα emission profiles. Furthermore, out of the 10 radio galaxies smaller than 50 kpc, strong H I absorption is found in 9 of them. The absorption gas appears to have a covering factor near unity over very large scales, namely as large as the underlying emission gas.

The current paper addresses the problem of the ionization state of both the absorption and the emission gas as well as the interconnection between the two. The main justifications behind this work are the following: HZRG are probably the progenitors of the massive central cluster galaxies (Pentericci et al. 1999) and as such are an important means by which we can study large ellipticals and their environment at such high redshift, a time not so long after, or even during their formation. Furthermore, the extended gas as detected in C IV (see below) is chemically enriched and therefore represents debris of past intense stellar formation periods and is interesting to study in their own right. What is the fate of such gas? How quickly has the enrichment of this large scale gas proceeded? Will this gas be heated up into a hot wind and enrich the intergalactic X-ray gas in cluster of galaxies? Will it on the contrary condense into sheets or condensations? A better understanding of the various gaseous phases which co-exist in high redshift objects would help anwering these questions.
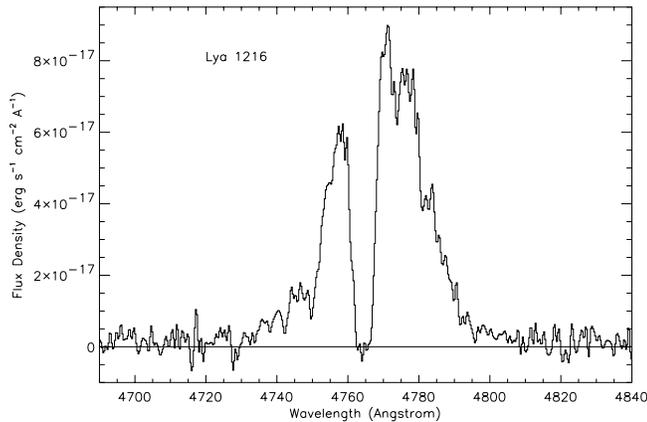
Fig. 1. An expanded plot of the Lyα spectral region obtained by RO95. The H II emission gas redshift is $z_e = 2.9233 \pm 0.0003$ and the main absorber of column $N_{HI} = 10^{19.0\pm0.2}$ cm^{-2} lies at $z_a = 2.9200 \pm 0.0002$.

To determine the physical conditions of the absorption gas, new observations were carried out at the wavelength of C IV and He II in 0943–242, the first radio galaxy reported to show large scale absorption troughs (Röttgering et al. 1995, hereafter RO95). The new spectrum shows the C IV absorption doublet at the same redshift[1] z_a as the Lyα absorption trough (RO95). Clearly and surprisingly the gas in absorption is highly ionized and probably of comparable excitation to the gas seen in emission.

This paper is structured as follows. We first present observations which show C IV in absorption in 0943–242 (Sect. 2). In Sect. 3 we derive a ratio (Γ) relating the observed emission and absorption quantities which depends somewhat on the ionization fraction of H but not explicitly on the C/H metallicity ratio. At first, we postulate that the emission and absorption gas components are co-spatial and share the same excitation mechanism and physical conditions and proceed to model Γ with a one-zone equilibrium photoionization model. We improve on the model using a stratified photoionized slab. As the observed ratio cannot be reproduced even in the case of collisional ionization, we discuss in Sect. 4.1 two alternative interpretations of this significant discrepancy. We demonstrate the many advantages of the winning scenario in which the absorption gas is further out and of much lower density, pressure and metallicity than the emission gas.

2. Observations of C IV (and Lyα) in absorption in 0943–242

2.1. Earlier observations of 0943–242 at $z_e = 2.92$

The low resolution spectrum of 0943–242 shown in RO95 and discussed also in van Ojik et al. (1996) displays the characteristic emission lines of a distant radio galaxy: strong Lyα, weaker C IV, He II and possibly C III]. This object was also observed

---

[1] We will distinguish between absorption and emission redshifts using subscripts, as in z_a and z_e, respectively.

at intermediate resolution (1.5Å) by RO95 in the region of Lyα with the slit positioned along the radio axis. The initial discovery of extended absorption troughs was based on this latter spectrum which we reproduce in Fig. 1.

2.2. New observations of C IV and He II at intermediate resolution

With the objective of providing constraints on the abundances and kinematics of the gas in 0943–242, sensitive high-resolution spectroscopic observations centered at the C IV and He II lines were performed at the Anglo Australian Telescope (AAT) on 1995 March 31 and April 1 under photometric conditions and with a seeing which varied from $1''$ to $2''$. The RGO spectrograph was used with a 1200 grooves mm^{-1} grating and a Tektronix 1024^2 thinned CCD, yielding projected pixel sizes of $0.79'' \times 0.6$Å. The projected slit width was $1.3''$, resulting in a resolution as measured from the copper-argon calibration spectrum of 1.5Å FWHM; the slit was oriented at a position angle of $74°$, i.e. along the radio axis (as in RO95).

The total integration time of 25000s was split into 2×2000s and 7×3000s exposures in order to facilitate removal of cosmic rays. Exposure times were chosen to ensure that the background was dominated by shot noise from the sky rather than CCD readout noise. Between observations the telescope was moved, shifting the object slit by about 3 spatial pixels, so that for each exposure the spectrum was recorded on a different region of the detector. The individual spectra were flat-fielded and sky-subtracted in a standard way using the long-slit package in the NOAO reduction system IRAF. The precise offsets along the slit were determined using the position of the peak of the spatial profile of the C IV and He II lines. Using these offsets, the images were registered using linear interpolation and summed to obtain the two-dimensional spectrum. The resultant seeing in the final two-dimensional spectrum, measured from two stars on the slit, was $1.5''$ FWHM. The corresponding FWHM of C IV emission along the slit was $2.2''$, giving a deconvolved (Gaussian) width of $1.6''$ or 12 kpc. Within the errors, this is the same as that found for Lyα emission by RO95.

The two-dimensional spectrum was weighted summed over a 7 pixel ($5''$) aperture to obtain a one-dimensional spectrum. In Fig. 2 we show the AAT data in the form of a full-resolution spectrum.

2.3. Profile fitting of the emission and absorption Lyα and C IV lines

One deep trough is observed in the Lyα emission line (Fig. 1) which was interpreted as a large scale H I absorber by RO95. In addition there are a number of weaker troughs, presumably due to weak H I absorption. Fitting the emission line by a Gaussian and the H I absorption by Voigt profiles, RO95 infer a column density N_{HI} of $10^{19.0\pm0.2}$ cm^{-2} for the deep trough, a redshift $z_a = 2.9200 \pm 0.0002$ and a Doppler parameter b of 55 ± 5 km s^{-1}. For the three shallow troughs, they find N_{HI} ranging from $10^{13.8}$ to $10^{14.1}$ cm^{-2} and b ranging from 7 to 100 km s^{-1}.
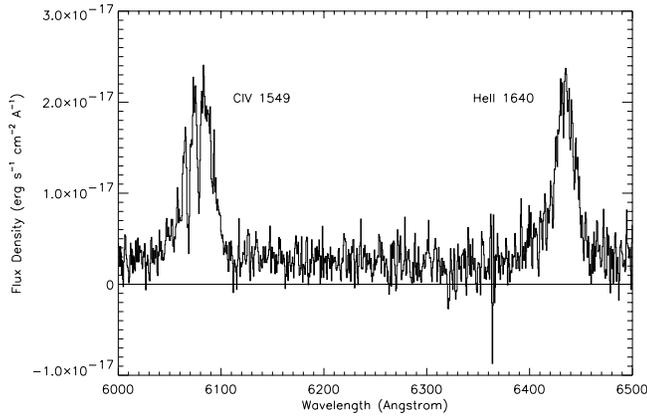
Fig. 2. The full-resolution AAT spectrum showing the C IV $\lambda\lambda$1548, 1551 and He II λ1640 lines.
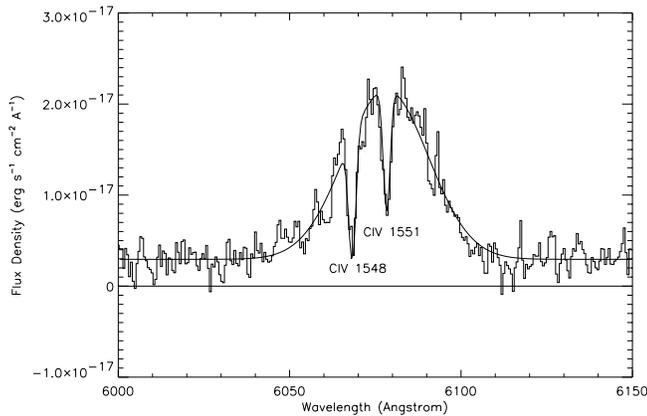

Fig. 3. An expanded plot of the full-resolution spectrum with the fit superimposed (solid line).

The redshift difference of the absorbers relative to systemic velocity when converted into inflow/outflow velocities indicate values not exceeding 800 $\mathrm{km\,s^{-1}}$. Because at the bottom of the main trough no emission is observed, the covering factor of the absorbing gas must be equal or larger than unity over the complete area subtended by the Lyα emission, indicating that the spatial scale of the absorber exceeds 13 kpc. This work will concern only the deep absorption trough.

To parameterize the C IV profile we have assumed that the underlying emission line is Gaussian, with Voigt profiles due to the C IV doublet absorption superimposed. We used an iterative scheme that minimizes the sum of the squares of the difference between the model and the observed spectrum, thereby solving for the parameters of the model (e.g. Webb 1987, vO97). Initial values were assumed for the shape of the Gaussian profile and the redshift of the absorber.

In Fig. 3 we show a portion of the spectrum with the model fits superimposed. The Gaussian fitted to the C IV emission line peaks at $z_e = 2.9247 \pm 0.0003$ and has a FWHM of 29 ± 2Å. We have corrected all wavelengths to the vacuum heliocentric system ($\simeq$+1.13 Å) before computing the redshifts. The two troughs in this figure correspond to the C IV $\lambda\lambda$1548, 1551 doublet produced by the same absorption system. Therefore, within

Table 1. Parameters for the Gaussian and Voigt profile fits

Emission	C IV	He II
Offset (10^{-17} erg cm^{-2} s^{-1})	0.29 ± 0.01	0.32 ± 0.07
Peak (10^{-17} erg cm^{-2} s^{-1})	1.90 ± 0.1	1.75 ± 0.2
Position of peak (Å)	6078.2 ± 0.5	6434.5 ± 0.5
z_e	2.9247 ± 0.0003	2.925 ± 0.001
FWHM ($\mathrm{km\,s^{-1}}$)	1430 ± 50	1025 ± 45
Absorption	**C IV**	
z_a	$2.9202 \pm .0002$	
$b\,(\mathrm{km\,s^{-1}})$	45 ± 15	
N_{CIV} (cm^{-2})	$10^{14.5\pm0.1}$	
Position of 1$^{\mathrm{st}}$ trough (Å)	6068.2	
Position of 2$^{\mathrm{nd}}$ trough (Å)	6078.3	

the fitting procedure, the wavelength separation and the ratio of the two profiles' depths are fixed by atomic physics while the two values for b are set to be equal. The fit gives for the location of the bottoms of the two troughs $\lambda = 6068.2$ and 6078.3Å resulting in a redshift of 2.9202 ± 0.0002. Within the errors this redshift is equivalent to that of the main H I absorber and in the subsequent analysis we will assume that the Lyα and C IV *absorption* gas belongs to the same absorber. We derive a Doppler parameter b for the doublet of $45 \pm 15\,\mathrm{km\,s^{-1}}$ and a column density N_{CIV} of $10^{14.5\pm0.1}$ cm^{-2} as summarized in Table 1.

As expected, He II appears only in emission without any absorption since it is not a resonance line. Parameters for the He II emission profile were obtained by fitting a Gaussian using the same iterative scheme (see Fig. 1 in Röttgering & Miley 1997). The peak is positioned at $z_e = 2.925 \pm 0.001$ and has a FWHM of 22 ± 2Å. The fitted parameters of the emission and absorption profiles are presented in Table 1. We recall that the FWHM of the Lyα emission profile is $1575 \pm 75\ \mathrm{km\,s^{-1}}$ (vO97), significantly larger than that of He II (see Table 1). Inspection of the various profiles in Fig. 1 and Fig. 2 (or Fig. 3) suggests the presence of an excess flux on the blue wings of all the emission profiles. Combining information from all the emission lines, our best estimate of the emission gas redshift is $z_e = 2.924 \pm 0.002$.

2.4. Velocity shear and subcomponents

To investigate whether there is any velocity shear in the C IV emission profile we fitted spatial Gaussian profiles to the emission line as a function of wavelength. In Fig. 4 we show the wavelength maxima of these spatial profiles and a line fitted through these points. The spatial profile of the C IV emission spectrum is displaced by $0.2''$, corresponding to a displacement of 1.5 kpc, over a wavelength range of 50Å. RO95 measured a comparable shift for Lyα of 1.8 kpc[2] although it appears that the latter displacement is due to a far more pronounced and abrupt difference in locations of the Lyα peak on both sides of the absorption trough. As Fig. 4 shows, the peaks of C IV emission

---

[2] This new value of $0.33 \pm 0.06\,\mathrm{pixels} \times 0.74\,\mathrm{arcsec/pixel} = 0.2442\,\mathrm{arcsec} \times 7.36\,\mathrm{kpc/arcsec} = 1.80 \pm 0.33\,\mathrm{kpc}$ is to be preferred to that quoted by RO95 of 2.5 kpc.
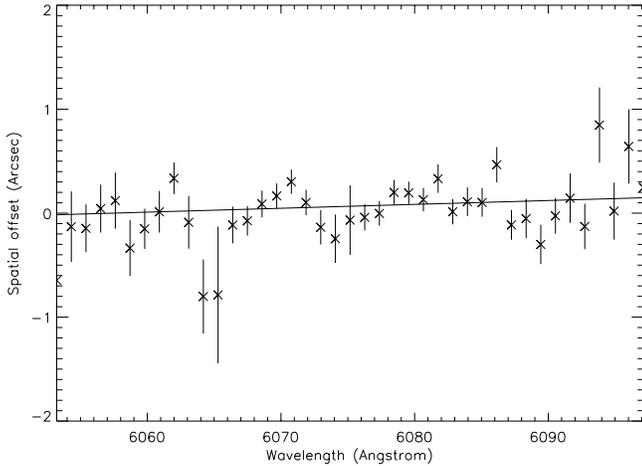
Fig. 4. The relative location of the peak of the C IV emission at constant wavelength as a function of wavelength. The line is a weighted fit to these peaks. The zero offset is arbitrary.

form a wavy line. We believe the velocity shear in the CIV profile to be less significant than the shear in the Lyα profile. We cannot rule out that the small velocity shear might be masking a possible break up of the absorption regions into a few saturated absorption components of smaller b.

A concern about the determination of N_{CIV} is the possibility that that there exist subcomponents in the absorption systems that have high column densities but low b values and are, therefore, not acounted for whenever individual velocity subcomponents are not resolved. Although we cannot strictly exclude this possibility, we adopt the stand of Jenkins (1986) and Steidel (1990a) who, using extensive absorption line studies, argue that this is unlikely to be the case, at least for C IV, and that a single-component curve-of-growth analysis can be used to infer total columns although the inferred *effective* b value has no physival meaning in terms of temperature. It is interesting to note that the physical conditions inferred from the C IV fit are fully consistent with the observed ratio of the doublet (since both troughs are equally well fitted). If the underlying continuum was flat, the N_{CIV} column and the b value we infer would imply a theoretical ratio of equivalent widths of $W_0(1548)/W_0(1551) = 1.4$, which is where the curve of growth just begins to leave the linear part (Steidel 1990a). Clearly the N_{HI} column might be susceptible to a larger error since Lyα is saturated. With these caveats in mind, we will assume in the following analysis that the adopted columns do not lie far off from reality.

3. A simple model for the ionized gas in emission and absorption

Our initial hypothesis is that the absorption gas is a subcomponent of the emission gas, sharing the same excitation mechanism and metallicity. We discuss the physical conditions of such gas and proceed to calculate an observable quantity, Γ, against which to compare the information provided by the Lyα and C IV lines in 0943–242.

3.1. Relation between the ionized absorption and emission components

The C IV and Lyα lines are both resonant lines and therefore prone to be seen in absorption against a strong underlying source. This property has consequences for the emission gas as well. In effect, for a geometry consisting of many condensations for which the cumulative covering factor approaches unity, the resonant line photons must scatter many times in between the condensations before they can escape. In this case, the emerging flux of any resonant line from a non uniform distribution of gas will not in general be an isotropic quantity but will depend on geometrical factors and on the relative orientation of the observer, a point which we now develop further.

We propose that some kind of asymmetry within the emission gas distribution can explain how a fraction of the ionized gas can be seen in absorption against other nearby components in emission. Let us suppose that the emission region is composed of low filling factor ionized gas condensations which are denser (therefore brighter) towards the nuclear ionizing source. In this picture, the Lyα or C IV photons are generated within and escape from such condensations, after which they start scattering on the surface of neighboring condensations until final escape from the galaxy (we assume that the cumulative covering factor is unity). Let us now suppose an asymmetry[3] in the global distribution of the outer condensations respective to the plane of the sky. In this case, the total number of scatterings on neighboring condensations before final escape will differ depending on the perspective of the absorber. Since for an observer situated on the side with an excess of condensations many of the resonant photons would have been 'reflected' away, we expect that the reduced flux would appear as an absorption line at the same velocity as that of the condensations responsible for reflecting away the resonant photons. The outer condensations (responsible for the absorption) must necessarily be of lower density in order to be of negligible emissivity respective to the inner (denser and therefore brighter) emission gas, otherwise the outer gas would out-shine in emission!

We should point out that for a density of the absorption gas as high as $100\,\mathrm{cm}^{-3}$ as argued for in vO97, such a gas cannot be photoionized by the metagalactic background radiation which would be much too feeble to produce C IV. The ionization to such a degree of the absorption gas is in itself puzzling. We adopt as working hypothesis that it is –similarly to the emission gas– photoionized by the AGN or by the hard radiation from photoionizing shocks.

Finally, the fact that both the absorption and emission gas contain a significant amount of C^{+3} argues in favor of a common geometry and excitation mechanism for the gas, the underlying hypothesis behind the calculations developed below.

---

[3] The asymmetry would take place either in space or in velocity domain or both.

3.2. The observable quantity Γ

The quantities determined from observation of 0943–242 are the following: the emission line ratio measured by Röttgering et al. (1997) is $\frac{I_{CIV}}{I_{Ly\alpha}} = 0.194$. We adopt the value of 0.17 following estimation of the missing flux due to the absorption troughs. As for the absorption gas, the H I and C IV column densities are 10^{19} cm^{-2} and $10^{14.5}$ cm^{-2}, respectively, as discussed in Sect. 2. These four quantities carry information on the three ionization species H^0, H^+ and C^{+3}. We define the ratio Γ as the following product of the emission and absorption ratios:

$$\Gamma = \frac{I_{CIV}}{I_{Ly\alpha}} \frac{N_{HI}}{N_{CIV}} = 0.17 \frac{10^{19.0}}{10^{14.5}} \simeq 5400 \qquad (1)$$

where N_{HI}/N_{CIV} is the ratio of the measured absorption columns. If, as postulated above, the gas responsible for absorption is simply a subset of the line emitting gas, the ratio Γ does not explicitly depend on the abundance of carbon as shown below.

3.3. The simplest case of an homogeneous one-zone slab

To compute Γ, in a first stage let us consider an homogeneous slab of thickness L of uniform gas density, temperature and ionization state to represent both the gas in emission and in absorption. Ignoring any peculiar scattering effects, the emission line ratio $\frac{I_{CIV}}{I_{Ly\alpha}}$ is given by the ratio of the local emissivities $j_{CIV}/j_{Ly\alpha}$ since the slab is homogeneous. For the emissivity of the C IV line, we have

$$4\pi j_{CIV} = 8.63\,10^{-6}\,h\nu_{C_{iv}}\,n_e n_{CIV}$$
$$\times \frac{\Omega_{C_{IV}}}{\omega_1}\exp\left(-h\nu_{CIV}/kT\right)/\sqrt{T} \qquad (2)$$

(Osterbrock 1989) where T is the temperature, $\Omega_{C_{IV}}$ the collision strength of the combined doublet, ω_1 the statistical weight of the ground state and $h\nu_{CIV}$ the mean energy of the C IV excited level. For the Lyα emissivity, we have

$$4\pi j_{Ly\alpha} = h\nu_{Ly\alpha}\,n_e n_{HII}\,\alpha_{2p}^{eff}(T) \qquad (3)$$

where α_{2p}^{eff} is the effective recombination coefficient rate to level $2p$ of H (Osterbrock 1989). By putting the temperature dependence and all the atomic constants in the function $f(T)$, the emission line ratio becomes:

$$\frac{I_{CIV}}{I_{Ly\alpha}} = \frac{Z_C^{emi}n_H\eta_{CIV}}{n_H y_{HII}}f(T) \qquad (4)$$

where n_H is the total hydrogen density, Z_C^{emi} the carbon abundance relative to H of the emission gas, η_{CIV} the fraction of triply ionized C and y_{HII} the ionization fraction of H.

The ratio of column densities N_{HI}/N_{CIV} can be written as:

$$\frac{N_{HI}}{N_{CIV}} = \frac{n_H x_{HI}}{Z_C^{abs}n_H\eta_{CIV}} \qquad (5)$$

where x_{HI} is the neutral fraction of H inside our homogeneous slab and Z_C^{abs} the carbon abundance of the *absorption* gas. As

we are testing the case which equates the absorption gas with the emission gas, then $Z_C^{abs} = Z_C^{emi}$. We denote as Γ the product of the two calculated ratios:

$$\Gamma = \frac{I_{CIV}}{I_{Ly\alpha}} \frac{N_{HI}}{N_{CIV}} = \frac{x_{HI}}{y_{HII}}f(T). \qquad (6)$$

We note that Γ is not directly dependent on either the abundance of C or on its ionization state. It is, however, dependent on the temperature and on the ionization state of H through the ratio[4] $\frac{x_{HI}}{y_{HII}}$. To compute this ratio, it is necessary to postulate an excitation mechanism. For this purpose, we have used the code MAPPINGS Ic (Binette, Dopita & Tuohy 1985; Ferruit et al 1997) to compute $\frac{x_{HI}}{y_{HII}}$ under the assumption of either collisional ionization or photoionization. Here are the results.

1. *Photoionization.* Putting in the atomic constants and calculating the equilibrium temperature and $\frac{x_{HI}}{y_{HII}}$ in the case of photoionization by a power law of index α ($F_\nu \propto \nu^\alpha$) of either -0.5 or -1, we find that the calculated Γ always lies within the range 0.8–12. The explored range in ionization parameter[5] U covered all the values which produce significant C IV in emission (C IV$/C > 8\%$), that is $10^{-3.5} < U < 10^{-1}$.

2. *Collisional ionization.* In this sequence of models, we calculated the ionization equilibrium of a plasma whose temperature varied from 30 000 K to 50 000 K. We find that Γ remains in the similar low range of 6–13. At the lower temperature end, Lyα emission is enhanced considerably by collisional excitation, which contributes in reducing Γ.

3. *Additional heating sources.* To cover the case of photoionization at a higher temperature than the equilibrium value (due to additional heating sources such as shocks), we artificially increased the photoionized plasma temperature to 40 000 K or 50 000 K for calculations with the same values of U as above. This did not extend the range of Γ obtained.

We conclude that for the simple one-zone case, Γ consistently remains below the observed value by more than two orders of magnitude.

3.4. The ionization stratified slab

To verify whether a stratified slab geometry might alter the above discrepancy in Γ, we have calculated in a similar fashion to Bergeron & Stasińska (1986) and Steidel (1990b) the internal ionization and temperature structure of a slab photoionized by radiation impinging on one-side (i.e. one-dimensional "outward only" radiation transfer) using the code MAPPINGS Ic. We adopted a power law of index $\alpha = -1$ as energy distribution. Since the column densities of H and C are useful diagnostics on their own right, we present in Fig. 5 the value of Γ for a slab as

---

[4] For all practical purposes, the high ionization regime under consideration implies that $y_{HII} = 1$.

[5] We use the customary definition of the ionization parameter $U = \varphi_H/n_H$ as the ratio between the density of ionizing photons (impinging on the slab) and the total H density at the face of the slab.
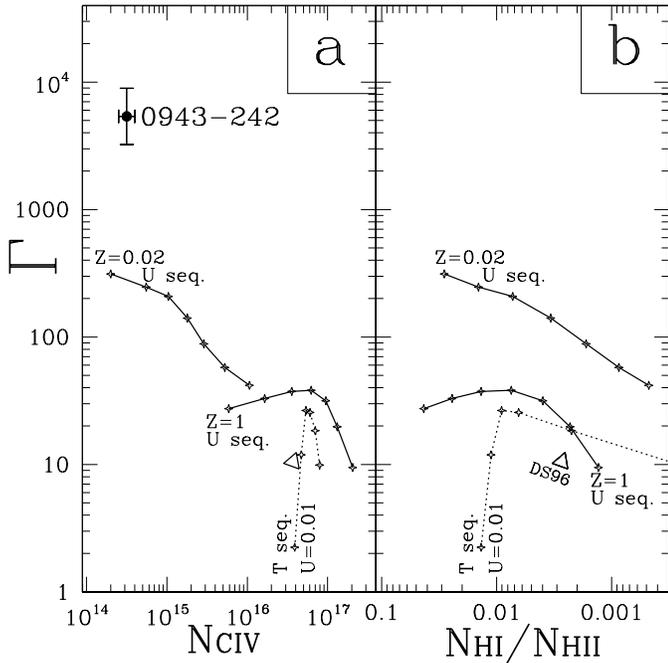
Fig. 5a and b. a Calculated and observed Γ as a function of the column density N_{CIV}. The filled circle represents the observed value for 0943–242. **b** The same models as a function of the column ratio N_{HI}/N_{HII}. In both panels, the solid line represents a sequence of photoionized slabs with U increasing from left to right, starting at $10^{-2.5}$. The gas total metallicity is either solar ($Z = 1$) or 1/50th solar. The separation between tick marks corresponds to an increment of 0.25 dex in U. All slab calculations were truncated at a depth corresponding to the observed $N_{HI} = 10^{19}$ cm^{-2}. The slab total column or N_{HII} can be inferred from panel b. [If we were to reduce by 100 the abundance of the absorption gas while keeping solar the emission gas ($Z_C^{abs}/Z_C^{emi} = 0.01$, see Eqs. 4 and 5), this would be equivalent to translating by 2 dex both up and to the left the $Z = 1$ sequence of panel a.] The dotted line represents a sequence of slabs of arbitrary uniform temperatures (all with $U = 10^{-2}$ and $Z = 1$) covering the range 10 000 K to 40 000 K (from left to right) by increments of 0.1 dex in T. The open triangle represents a slab photoionized by a high velocity shock of $V_{shock} = 500$ km s^{-1} from Dopita & Sutherland 1996.

a function of N_{CIV} (left panel) and N_{HI}/N_{HII} (right panel). (One can interpret N_{HI}/N_{HII} of Panel b as the mean neutral fraction of the slab: $\langle x_{HI}/y_{HII}\rangle$.)

The solid line in Fig. 5 represents a sequence of different slab models with increasing ionization parameter from left to right covering the range $10^{-2.5} \leq U \leq 10^{-1}$ for a gas of either solar metallicity ($Z = 1$) or with a significantly reduced metallicity of 1/50th solar. The practical constraint that C IV be a strong emission line implies that $U \geq 10^{-2.5}$. In all calculations, the thickness of the slab is set by the observable condition that $N_{HI} = 10^{19}$ cm^{-2}. Interestingly, such parameters result in a slab which in all cases is "marginally" ionization-bounded with less than 10% of the ionizing photons *not* absorbed.

The monotonic increase of the N_{CIV} column with U is in part due to the increasing fraction of C IV but mostly it is the result of the slab getting thicker (larger N_{HII} at constant

N_{HI}) since x_{HI} decreases monotonically throughout the slab with increasing U. The slope or curvature of the two solid lines reflect changes in the internal temperature stratification of the slab with increasing U. Because of the dependence of Γ on T (see Eq. 6), there exists an indirect dependence of Γ on the *total* metallicity given that the equilibrium temperature is governed by collisional excitation of metal lines (when $Z \gg 0.005$).

The striking result from the slab calculations in Fig. 5 is that the models with solar metallicity are still two order of magnitudes below the observed Γ. Another way of looking at this discrepancy is to consider separately the $\frac{I_{CIV}}{I_{Ly\alpha}}$ emission ratio or the $\frac{N_{HL}}{N_{CIV}}$ column ratio. Forgetting Γ, just to achieve the observed column of N_{CIV} ($10^{14.5}$ cm^{-2}), one would have to use a gas metallicity below solar by a factor $\gtrsim 50$ (see sequence with $Z = 0.02Z_\odot$), which cannot be done without irremediably weakening the C IV *emission* line to oblivion. Alternatively, reducing U much below $10^{-2.5}$ in the solar case can reproduce the N_{CIV} column but again the C IV *emission* line would be totally negligible.

Might the observed $\frac{I_{CIV}}{I_{Ly\alpha}} = 0.17$ emission line ratio be anomalous? This is not the case as the observed value in 0943–242 is typical of the value observed in others HZRG without, for instance, any evidence of dust attenuation of Lyα. This ratio is also that expected from photoionization models if a sufficiently high value of U is used (Villar-Martín et al. 1996).

Another possibility to consider is the presence of other heating sources such as shocks which would increase the temperature above the equilibrium temperature given by photoionization alone. Alternatively, small condensations in rapid expansion would result in strong adiabatic cooling and the temperature would be less than given by cooling from line emission alone. To explore such cases, we have calculated various isothermal photoionized slabs of different (but uniform) temperatures (all with $U = 10^{-2}$). They cover the range 10 000–40 000 K and are represented by the dotted line in Fig. 5. These models are in no better agreement with respect to Γ. (Varying U for any of these isothermal temperature slabs would result in an horizontal line). We also computed Γ for a solar metallicity (precursor) slab submitted to the ionizing flux of a 500 km s^{-1} photoionizing shock (Dopita & Sutherland 1996). This model which is represented by an open triangle in Fig. 5 does not fare better than the power law photoionization models.

4. Discussion

4.1. Interpretation of the large Γ

What is the significance of the obvious discrepancy between models and the observed Γ? Clearly, the working hypothesis that the emitting and absorption gas phases are physically the same, is now ruled out and an alternative explanation must be sought for, based on our result that the two gas phases (absorption vs. emission) are physically distinct. We consider the two following explanations in Sects. 4.1.1 and 4.1.2.

4.1.1. The absorption gas is metal-poor and further out

Since the absorption gas in this picture is not spatially associated with the emission gas, its metallicity is unconstrained. It turns out that the value of $\Gamma \simeq 5400$ is easily reproduced by simply using $Z_C^{abs}/Z_C^{emi} \sim 0.005$ in the one-zone case (see Eqs. 4 and 5). The more rigorous stratified slab geometry would favor a value of $Z_C^{abs}/Z_C^{emi} \sim 0.01$ to reproduce the same Γ, assuming both gas phases to have equal excitation. Can we disentangle the absolute abundance values? We cannot rely on the emission spectra alone to derive a precise and independent value for Z_C^{abs} as the emission lines are very model-dependent, with fluxes from lines like C IV depending critically on the temperature. It can realistically be argued, however, that a Z_C^{emi} less than half solar could *not* reproduce the observed metal line ratios. On the other hand, a Z_C^{emi} much higher than solar cannot be ruled out in absence of direct knowledge of the ionizing continuum distribution. We consider more plausible a near solar value for Z_C^{emi} on the ground that the extended emission lines extend over 13 kpc and therefore sample a huge galactic region very distinct from that of the nucelar BLR (hidden here) which has been shown to be ultra-solar in high z QSOs (Hamann & Ferland 1999 and references therein). An attempt, on the other hand, to model separately the absorption columns observed in 0943–242 as described below in Sect. 4.2 is more dependable since temperature is much less of an issue. The value inferred below of $Z_C^{abs} \sim 0.01 Z_\odot$ is consistent with those observed in absorbers of comparable redshift along the line of sight of more distant QSOs (Steidel 1990a). Since measured galactic metallicity gradients are always negative and a function of the distance to the nucleus, such a contrast in metallicity between absorption and emission gas makes more sense if the absorption gas is located much further out than the emission gas which extends to at least 13 kpc in 0943–242.

We emphasize that this scenario does not entail that the absorption gas does not belong to the environment of the parent radio galaxy. As argued by vO97, the high frequency of detection of H I aborbers in 9 out of 10 radio galaxies *smaller* than 50 kpc, much in excess of the density of absorbers along any line of sight to distant QSOs, is a compelling argument for concluding that the absorption gas is spatially related to the parent galaxy. Our postulate is that the large scale H I *absorption* gas is the same gas which is seen instead in *emission* in those radio galaxies with Lyα sizes *larger* than 50 kpc. In effect, absorption troughs are not seen when the emission gas extends beyond 50 kpc. Such objects in general also have much larger radio sizes as shown by vO97. Kinematically, the gas which is seen in emission at the largest spatial scales shows narrow FWHM. For instance a reresentative case is the radio galaxy 1243+036 ($z_e = 3.57$) which was studied in great detail by van Ojik et al. (1996) and which reveals the presence of very faint Lyα emission extending up to 136 kpc, a region labelled "outer halo". This emission gas has a FWHM of 250 km s^{-1} and shows clear evidence for rotational support.

A straightforward explanation of why the same gas is seen in emission in some objects while in absorption in others might simply be the environmental pressure. A larger pressure, like the one adopted by vO97 can cause the warm gas to condense and hence reduce his filling factor as compared to similar gas components in a low pressure environment. Due to this process, high pressures and consequently high densities lead to detectable Lyα since emissivities scale proportionally to n_H^2, but also to an overall smaller covering factor (hence no detectable absorption) while low pressures lead to large covering factors (hence absorption) as well as negligible emissivities. Differences in pressure in the outer halo would therefore naturally account for the reported dichotomy of detecting H I troughs exclusively in those emission Lyα objects devoid of very large scale emission ($\lesssim 50$ kpc)

Since absorption troughs tend to be absent in radio galaxies showing the largest radio scales, we propose that the gas which is seen in absorption must lie *outside* the zone of influence of the radio jet cocoon, a region with pressure of order 10^6 K cm^{-3} (vO97). An unpressurized outer halo responsible for the absorption troughs ought to precede the regime in which the radio material has expanded sufficiently outward to pressurize the outer halo. The eventual increase in environmental pressure would either disrupt the gas or compresses it into small clumps (making it unobservable in absorption when the covering factor dwindles), which becomes visible in emission if it lies within the ionizing cone. vO97 assumed that the absorption and emission gas were both immersed in zones of comparable surrounding pressure ($n_H T \sim 10^6$ K cm^{-3}) and were therefore of comparable density (~ 100 cm^{-3} for a photoionized gas). We propose instead that whenever aborption troughs are observed, the absorption gas must lie outside the radio jet cocoon, allowing for a lower density and high covering factor.

The clear-cut advantages of locating the H I absorber in an unpressurized outer halo are threefold:

1. We can now get the high excitation of the low density absorption gas for free. In effect, if the density of the absorption gas is as low as 10^{-3}–10^{-2} cm^{-3}, the metagalactic background radiation suffices to photoionize the absorption gas to the high degree observed in 0943–242, whether it does or does not lie within the ionizing cone of the nucleus. Conversely, for the objects devoid of absorption, when a higher pressure has set in in the outer halo (as we presume to be the case in 1243+036), the gas is much denser and can be seen in emission only if it lies whithin the ionizing cone (since a high density gas of ~ 100 cm^{-3} cannot be kept highly ionized by the background metagalactic radiation). This picture would be in accord with the findings of van Ojik et al. (1996) who detect Lyα in emission in 1243+036 only along the radio axis (presumably the same axis as that of the ionizing radiation cone) and *not* in the direction perpendicular to it.

2. The much smaller velocity dispersion ($b \simeq 45$ km s^{-1}) of the absorption gas as compared to the emission gas (FWHM/2.35 $\simeq 600$ km s^{-1}, cf. Table 1) is more readily explained if the absorption gas lies undisturbed at relatively large distances from the parent galaxy.

3. It explains why the absorption (yet ionized) gas in 0943–242 is not seen in emission while being more massive than the inner emission Lyα gas observed within 13 kpc. In effect, the mass of ionized gas either in emission or absorption around 0943–242 inferred by vO97 are $1.4\,10^8$ M$_\odot$ and $10^7 (x_{HI}/y_{HII})^{-1}$ M$_\odot$, respectively. Adopting the conservative value of $\langle x_{HI}/y_{HII} \rangle \simeq 0.03$ (cf. panel b in Fig. 5), the total ionized mass of the absorption ionized gas therefore exceed that of the inner emission gas by at least a factor two and yet it is not seen in emission! This huge pool of ionized gas can remain undetectable in emission only if it has a very low density, as argued above. It is customary to assume a volume filling factor of 10^{-5} for the gas detected in emission in radio galaxies and that this gas is immersed in a region characterized by a pressure of order 10^6 K cm^{-3} (vO97; van Ojik 1996). If we suppose instances where the outer halo has much lower pressure than this, it can be shown that for the same outer halo mass, the luminosity in Lyα would scale inversely to the volume filling factor. Hence, the gas would be weaker in emission by a factor of 10^{-5} if its filling factor approached unity (with the mean density being lower by the same amount). This scheme would easily explain why the outer halo of 0943–242 is not seen in emission despite its huge mass (comparable incidentally to the outer halo mass measured in emission in 1243+036 of $2.8\,10^8$ M$_\odot$ by van Ojik et al. 1996).

4.1.2. A two-phase gas medium

Due to radiative cooling (which goes as n_H^2 and rise steeply with T), density enhancements can condense out of the emitting gas and form a population of about 100 times denser and 100 times cooler clouds in pressure equilibrium with the ambient medium. If we maintain that the pressure characterizing the absorption and the emission gas is comparable ($\sim 10^6$ K cm^{-3}) and that either gas phase has a temperature typical of photoionization, $T \sim 10^4$ K, we obtain (adopting a similar notation to vO97 but adapted to the case of 0943–242) that the size and the number of small *homogeneous* absorbing condensations required to cover the emission region would be $0.85 r_{03}$ pc and $2.4\,10^8 r_{03}^{-2}$ clouds, respectively, where $r_{03} = 0.03 \times \langle x_{HI}/y_{HII} \rangle^{-1}$ [as above we adopt 0.03 as the reference neutral H fraction]. Can we find an alternative interpretation to (1) above for explaining the large Γ that does not require low metallicities for the absorption gas? Such a possibility would arise if the N_{HI} column was not directly related to the N_{CIV} column. For instance, in the auto-gravitating absorber model of Petitjean et al. (1992), which consists of a self-gravitating gas condensation with a dense neutral core surrounded by photoionized outer layers, could in principle give ratios between columns of H I and C IV which do not reflect the abundance ratio but represents rather the average impact parameter for our line of sight. Of course, these models have to be rescaled to a pressure of $n_H T = 10^6$ K cm^{-3} implying much smaller sizes but requiring much higher ionizing fluxes (both by a factor $\sim 10^4$). This rescaling poses no conceptual problems if we assume that the photoionization is by the central AGN. Using their figures and Table 4 (Petitjean et al. 1992), we infer that the number of auto-gravitating condensations needed to achieve a covering factor of unity and a mean H I column of 10^{19} cm^{-2} would have to be large, in excess of $10^{9.5}$, for instance, for the model C$_{7000}^{10}$. However, after inspection of the various N_{CIV} columns derived from their extensive grid of models, we did not find any model which would reproduce the observed C IV column without having a metallicity $\leq 0.1 Z_\odot$. The gain in Z is therefore insufficient to get $Z_C^{abs} \simeq Z_C^{emi} > 0.5$ and we conclude that this explanation for a high Γ is unworkable.

4.2. Metallicity determination of the absorption gas

Our favoured interpretation of the large Γ is that the absorption gas is of very low metallicity compared to the (inner/denser) emission gas. Furthermore, a close parallel in the physical conditions of the absorption gas could be made with those adopted for the study of QSO absorbers (e.g. Steidel 1990a,b; Bergeron & Stasińska 1986), namely the densities, the metallicities and the excitation mechanism (photoionization by a hard metagalactic background radiation). The observed N_{HI} column of 10^{19} cm^{-2} would position the 0943–242 absorber in the category of "Lyman limit system" according to Steidel (1992). The coincidence in physical conditions might be fortuitous and it does not imply per se a common origin or correspondance between QSO absorbers and outer halos of radio galaxies. Under the sole assumption of similar physical conditions, what estimate of the metallicity can we derive for C? From the N_{CIV}/N_{HI} ratio, we cannot determine the ionization parameter and therefore directly apply the results and models of Steidel (1990b) who determined for each Lyman limit system a probable range of U from upper limits or from measurements of other species than C IV. It is nevertheless reasonable to assume that the excitation degree in 0943–242 is comparable to that encountered in high excitation QSO absorbers. To determine an appropriate value for U, we adopted the set of data provided by the three Lyman limit systems observed in the spectrum of the QSO HS1700+6416 by Vogel & Reimers (1993) who successfully measured the columns of up to 3–4 ionization species of each of the three elements C, N and O. Amongst our $\alpha = -1$ model sequence (Sect. 3.4), we selected the model which had the same U ($\simeq 0.007$) as Vogel & Reimers (1993) and inferred that the observed columns in 0943–242 implied that the Carbon metallicity of the absorption gas was 1% solar (that is C/H $\sim 4\,10^{-6}$), which is broadly consistent with the range of Z_C^{abs} values favored in Sect. 4.1.1.

4.3. Mean density and cloud sizes

What would be the minimum density assuming the absorption gas to be uniformly distributed? If our proposed picture was correct, a representative size for the absorption gas volume is that given by the outer halo as seen in emission in other HZRG. Let us adopt the value measured for 1243+036 by van Ojik et al. (1996) of 136 kpc. Assuming the same mean ionization parameter as used above (0.007), we derive a total gas column

of $N_H = N_{HII} \simeq 10^{21}$ cm^{-2}. Hence the mean density for a volume filling factor unity on a scale of the 1243+036 outer halo would be $\simeq 2\,10^{-3}$ cm^{-3} which is a value sufficiently low to allow photoionization by the feeble ionizing metagalactic background radiation.

4.4. Comparison with the metallicity of BAL QSOs

Our estimate of the metallicity for the outer halo of 0943–242 is at odds with the super-solar metallicities (e.g. Hamann 1997, Papovich et al. 2000) of the "associated" absorbers seen in high redshift QSOs. The QSO emission gas itself (the BLR) is similarly characterized by super-solar metallicities (cf. Hamann & Ferland 1999 and references therein). If we consider QSOs and HZRG as equivalent phenomena observed at different angles, it may appear at first surprising that the metallicities of the absorption components are so different. However, we show below that this contradiction is only apparent as we are probably dealing with totally different gas components.

1. *Kinematics.* The HZRG large scale absorbers are kinematically very quiescent. In effect, the modulus of the velocity offset between the absorbers and the parent galaxy is usually less than 400 km s^{-1} for the dominant absorber (vO97)[6]. A substantial fraction of HZRG absorbers are actually infalling (Binette et al. 1998). This is far from being the case for QSO "associated" absorbers whose ejection velocities can extend up to many thousands km s^{-1} (Hamann & Ferland 1999). For instance, the two associated systems (with detected metal lines) recently studied by Papovich et al. (2000) are blueshifted by -680 and $+4000$ km s^{-1}, respectively.

2. *Selection effect.* QSOs are spatially unresolved with a size of the source light beam less than a few light-weeks across. In the case of HZRG absorbers, the background source is the emission gas which extends over a scale ~ 35 kpc. This huge difference in scale results in a totally different bias on what is preferentially observed. In effect, the extended absorbers of HZRG are weighted towards the largest volumes and hence towards the most massive gas components (the total mass of the absorption component exceeds 10^8 M$_\odot$ in 0943–242). By contrast, in the case of QSO associated absorbers, the mass of gas directly seen in absorption is tiny (e.g. $\sim 4\,10^{-6}$ M$_\odot$ if one considers a background light beam one light-month diameter and a total gas absorption column of 10^{18} cm^{-2}).

3. *Coexistence with the BLR.* To the extent that QSO associated absorbers represent gas components expelled from the BLR, we should not be surprised that their metallicity turn out comparable to the BLR. Given that in HZRG we do not directly see the pointlike AGN, we cannot expect to see any BLR component in absorption. As for the extended gas detected in HZRG, there exists no evidence in favour of super-solar metallicities on large scales > 10 kpc (N V when detected is strong only in the nucleus) If a fraction of asso-

ciated absorbers correspond to intervening galaxies close to the QSO, we might expect to see amongst counterpart HZRGs one or more C IV or Lyα absorbers of small spatial extent relative to the size of the extended emission gas. The weak H I absorption found by Chambers et al. (1990) in 4C41.17 might be such occurrence given its partial coverage of the Lyα background.

We conclude that HZRG absorbers, when their size is comparable to galactic halos (as those found by vO97), have probably little to do with QSO associated absorbers. A more suitable analogy to the absorption gas of HZRG is that of the Francis cluster of galaxies at $z = 2.38$ which is characterized by large scale absorption gas on a scale of $\gtrsim 4$ Mpc (Francis et al. 2000).

4.5. Constraints on radio galaxy evolution

The size of the radio source can be used as a clock that measures the time elapsed since the start of the radio activity. A number of observed characteristics of distant radio galaxies change as a function of radio size, – i.e. as function of time elapsed (cf. Röttgering et al. 2000). For $z \sim 1$ 3CR radio sources, these include optical morphology (Best et al. 1996), degree of ionisation, velocity dispersion and gas kinematics (Best et al. 2000). At higher redshifts ($z > 2$), only the smaller radio galaxies are affected by H I absorption (vO97). All these observations seem to dictate an evolutionary scenario in which the radio jet has a dramatic impact on its environment while advancing on its way out of the host galaxy (Röttgering et al. 2000, Best et al. 2000).

5. Conclusions

The detection of C IV absorption in radio galaxy 0943–242 at the same redshift as the deep Lyα trough observed by RO95 demonstrates that the detected absorption gas is highly ionized. Having assumed that the H I and C IV columns measured from the Voigt profile fitting were representative of the dominant gas phase (by mass) in the outer halo, we have effectively ruled out that the absorption and emission gas occupy the same position in 0943–242. We subsequently reassessed the picture proposed by vO97 in which both the large scale emission gas and the absorption gas were of comparable density ($n_H \sim 100$ cm^{-3}). In the former picture, the absorption gas was believed to lie outside the AGN ionization bicone (see their Fig. 11 in vO97). To ionize the gas to such a degree without using the AGN flux is problematic. We have proposed an alternative picture in which the absorption gas is of very low metallicity and lies far away (in the outer halo) from the inner pressurized radio jet cocoon. Since in this new scheme the density of the absorption gas is expected to be very low, the metagalactic background radiation now suffices to photoionize it. Furthermore, the structure of the absorption gas is now drastically simplified since we do not need over $\sim 10^{10}$ condensations of size ~ 1pc and density $\sim 10^2$ cm^{-3} to reach a covering factor close to unity. We can now reach similarly high covering factor using a single or few shells of very low density which have a volume filling factor close to unity (assuming a density of $\sim 10^{-2.5}$ cm^{-3}).

---

[6] Highly blueshifted P-cygni profiles are now known to exist in radio galaxies with $z \geq 3.5$ (Dey 1999).

It appears to us that the low metallicity inferred ($Z \simeq 0.01 Z_\odot$) and the proposed location of the absorption gas in 0943–242 –outside the radio cocoon, in an outer halo which is seen in emission in other radio galaxies (as in 1243+036)– strongly suggest that the absorbers' existence precedes the observed AGN phase. Unless this non-primordial gas has been enriched by still undetected pop III stars, we consider that it more likely corresponds to a vestige gas phase expelled from the parent galaxy during the initial starburst at the onset of its formation.

If the C IV doublet was detected in absorption in other radio galaxies with deep Lyα absorption troughs, there are many aspects which would be worth studying. For instance, how uniform is the excitation of the absorption gas across the region over which it is detected? Is a single phase sufficient? This could be tested by an attempt to detect absorption troughs of Mg II $\lambda\lambda 2798$ or imaging the troughs in C IV with an integral field spectrograph on an 8-m class telescope. How different is the metallicity of the absorption gas in the other radio galaxies? The information gathered could then be used to infer the enrichment history of the outer halo gas which surrounds HZRG.

References

Bergeron J., Stasińska G., 1986, A&A 169, 1

Binette L., Dopita M.A., Tuohy I.R., 1985, ApJ 297, 476

Binette L., Joguet B., Wang J.C.L., Magris C.G., 1998, The Messenger 92, 36

Best P.N., Longair M.S., Röttgering H.J.A., 1996, MNRAS 280, L9

Best P.N., Röttgering H.J.A., Longair M.S., 2000, MNRAS 311, 23

Chambers K.C., Miley G.K., van Breugel W.J.M., 1990, ApJ 363, 21

Dey A., 1999, In: Best P.N., Lehnert M.D. (eds.) Proc. of the KNAW colloquium: The Most Distant Radio Galaxies. Amsterdam, 15-17 October, 1997, Amsterdam

Dopita M.A., Sutherland R.S., 1996, ApJS 102, 161 (DS96)

Ferruit P., Binette L., Sutherland R.S., Pécontal E., 1997, A&A 322, 73

Francis P.J., Wilson G.M., Woodgate B.E., 2000, ApJ submitted

Hamann F., 1997, ApJS 109, 279

Hamann F., Ferland G., 1999, ARA&A 37, 487

Jenkins E.B., 1986, ApJ 304, 739

Osterbrock D., 1989, In: Astrophysics of gaseous nebulae and active galactic nuclei. University Science Books, Mill Valley

Papovich C., Norman C.A., Bowen D.V., et al., 2000, ApJ in press (astro-ph/9910349)

Petitjean P., Bergeron J., Puget J.L., 1992, A&A 265, 375

Pentericci L., Röttgering H.J.A., Miley G.K., et al., 1999, A&A 341, 329

Pettini M., Hunstead R., Smith L., David, P.M., 1990, MNRAS 246, 545

Röttgering H.J.A., Hunstead R.W., Miley G.K., van Ojik R., Wieringa M.H., 1995, MNRAS 277, 389 (RO95)

Röttgering H.J.A., Miley G.K., 1997, In: Bergeron J. (ed.) The Early Universe with the VLT. Springer, Berlin, p. 285

Röttgering H.J.A., van Ojik R., Miley G.K., et al., 1997, A&A 326, 505

Röttgering H.J.A., Best P.N., de Breuck C., Kurk J., Pentericci L., 2000, In: van Haarlem M.P., van der Hulst J.M. (eds.) Proc. of Perspectives in Radio Astronomy: scientific imperatives at cm and mm wavelengths. in press

van Ojik R., Röttgering H.J.A., Carilli C.L., et al., 1996, A&A 313, 25 (vO96)

van Ojik R., Röttgering H.J.A., Miley G.K., Hunstead R.W., 1997, A&A 317, 358 (vO97)

Steidel C.C., 1990a, ApJS 72, 1

Steidel C.C., 1990b, ApJS 74, 37

Steidel C.C., 1992, PASP 104, 843

Villar-Martín M., Binette L., Fosbury R.A.E., 1996, A&A 312, 751

Vogel S., Reimers D., 1993, A&A 274, L5

Vogel S., Reimers D., 1995, A&A 294, 377

Webb J., 1987, Ph.D. Thesis, University of Cambridge (UK)